Validation of time-domain calibration

Eiichi Hirose[1], Xavier Siemens[2]
[1]Department of Physics, Syracuse University, Syracuse NY 13244
[2]Physics Department, California Institute of Technology, Pasadena, CA 91125
Feb 5, 2007 (Revised from a document on Sep 22, 2006)

ABSTRACT

We investigate a method for validation of time domain (TD) calibration. The basic idea is to see whether TD calibration can reproduce gravitational wave strain signals calibrated by frequency domain (FD) method. We use sine-Gaussian (SG) signals for artificial gravitational wave signals injected into S4 detector noise data and check if we get reasonable agreement between the two methods. The two methods agree to each other within 3.2 % in amplitude and 3 degree in broad frequency range (from 40Hz to 6000Hz). This document was prepared for LIGO Scientific Collaboration (LSC).

1. Introduction

There are two calibration methods in LIGO. One is frequency domain calibration [1] which has been historically used, and the other one is time domain calibration which is comparably new [2]. Figure 1 shows relation between the two domains.

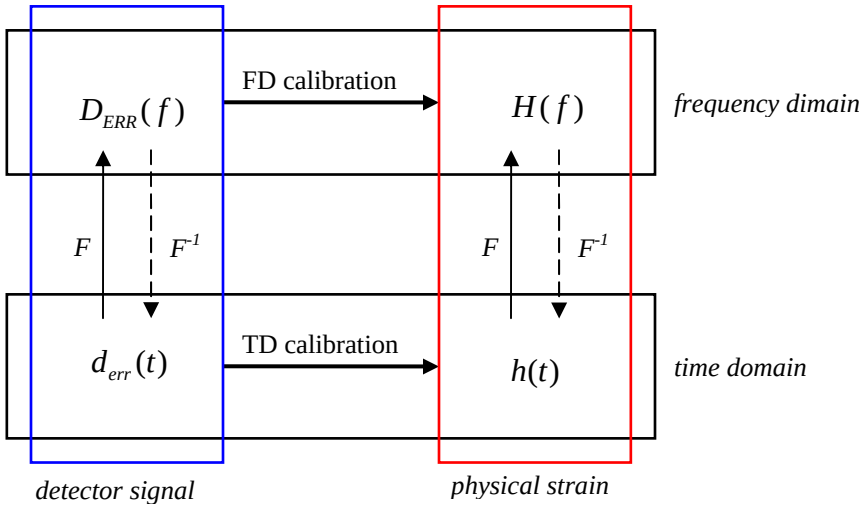

Figure 1: Conceptual diagram

F and F^{-1} in the figure are Fourier transform and inverse Fourier transform respectively. Mathematically, the two methods are related by the following equations.

$$H(f) = R(f)D_{ERR}(f) = F\left[\int_{-\infty}^{+\infty} r(t-t')d_{err}(t')dt'\right] \quad (1)$$

$$\therefore h(t) = F^{-1}\left[H(f)\right] = \int_{-\infty}^{+\infty} r(t-t')d_{err}(t')dt' \quad (2)$$

Here, $R(f)$ and $D_{ERR}(f)$ are Fourier transform of $r(t)$ and $d_{err}(t)$ respectively. $R(f)$ is so called response function, which is inverse of detector response to gravitational wave signals. FD calibration produces $R(f)$ while TD calibration makes $r(t)$ to get $h(t)$ directly from detector time series output. Whole idea of TD calibration is to digitize response function $R(f)$. The detail of each method can be found in [1] and [2],

2. Method

There must exist a couple of ways to compare the two methods. The most straightforward way would be to compare (3) with (4).

$$h_1(t) = F^{-1}[R(f)D_{ERR}(f)] = F^{-1}[R(f)F[d_{err}(t)]] \quad (3)$$

$$h_2(t) = \int_{-\infty}^{+\infty} r(t-t')d_{err}(t')dt' \quad (4)$$

However, since $d_{err}(t)$ usually (so far) does not contain gravitational wave signals but just contains detector noise, we thought it would be desirable to inject artificial gravitational wave signals when investigation takes place. Therefore, one validation method with artificial gravitational waves will be the following. First, we prepare an artificial gravitational strain signal $h(t)_{GW}$, which will be sine-Gaussian wave in this study. Using FD calibration inversely, a time series $d_{error}(t)_{GW}$ is obtained. Then, we add $d_{err}(t)_{GW}$ to $d_{err}(t)$ in order to embed a fake gravitational wave signal into detector noise signal. Applying TD calibration code for both the combined detector signal '$d_{err}(t) + d_{err}(t)_{GW}$' and pure detector noise $d_{error}(t)$, we get two strain time series $h(t)_{err+GW}$ and $h(t)_{err}$ respectively. Finally, subtracting $h(t)_{err}$ from $h(t)_{err+GW}$, we get a reconstructed gravitational signal $h_{rec}(t)$.

$$d_{err}(f)_{GW} = R^{-1}(f)h(f)_{GW} = R^{-1}(f)F[h(t)_{GW}] \quad (5)$$

$$d_{err}(t)_{GW} = F^{-1}[d_{err}(f)_{GW}] \quad (6)$$

$$h(t)_{err+GW} = \int_{-\infty}^{+\infty} r(t-t')\{d_{err}(t') + d_{err}(t')_{GW}\}dt' \quad (7)$$

$$\therefore h(t)_{rec} = h(t)_{err+GW} - h(t)_{err}$$

$$= \int_{-\infty}^{+\infty} r(t-t')\{d_{err}(t') + d_{err}(t')_{GW}\}dt' - \int_{-\infty}^{+\infty} r(t-t')d_{err}(t')dt' \quad (8)$$

Subtraction (8) makes the comparison 'ideal' because it kills influence coming from detector noise. Namely, this test purely extracts systematic difference between the two calibration

methods. If everything is perfect, which is not likely however, we can continue calculation (8) in the following way.

$$\int_{-\infty}^{+\infty} r(t-t')\{d_{err}(t') + d_{err}(t')_{GW}\}dt' - \int_{-\infty}^{+\infty} r(t-t')d_{err}(t')dt' \\ = \int_{-\infty}^{+\infty} r(t-t')d_{err}(t')_{GW}\,dt' = h_{GW}(t) \qquad (9)$$

Thus, the program of this study is to see the difference between $h(t)_{rec}$ and $h(t)_{GW}$, or difference between (8) and (9). If $h_{rec}(t)$ perfectly coincides with the original sine-Gaussian signal $h(t)_{GW}$, it will be the case that TD calibration perfectly produces the same strain as frequency domain calibration does. There is, of course, some discrepancy, and it will be discussed in chapter 3.

2. Details

2-1. Sine-Gaussian signals

We used sine-Gaussian (SG) as fake gravitational wave signals. Plotted in figure 2 is a SG waveform, whose center frequency is 235Hz and Q values is 9.

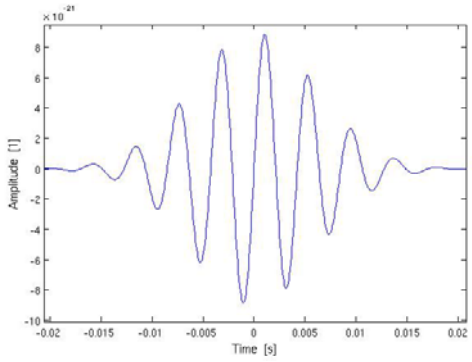

Figure 2: A sine-Gaussian wave form ($f_0 = 235Hz,\ h_0 = 0.9\times10^{-20}$)

SG is described in the following equation.

$$h = h_0 \sin(2\pi f_0 t)\exp\left(-(t/\tau)^2\right) \quad , \ where \quad \tau = \left(Q/\sqrt{2}\pi f_0\right) \qquad (10)$$

Six different waveforms used in this study are listed in table 1. We chose center frequency from 100Hz to 4000Hz and amplitude from 9.0×10^{-21} to 2.3×10^{-20}. The selection was made after some trial and error to cover entire frequency region in which we are interested.

h_0	f_0	Q
9.00E-21	100	8.9
9.00E-21	235	8.9
1.30E-20	554	8.9
2.30E-20	849	8.9
9.00E-21	2000	8.9
9.00E-21	4000	8.9

Table 1: Parameters of the sine-Gaussian waves

2-2. Real noise data

The artificial gravitational signals are added to real detector noise signal $d_{err}(t)$, H-R_cit_LDAS_CIT2373460-795934848-32.gwf. The length is 32 second starting at GPS time 795934848. In this period, H1 is in science mode and no hardware injection took place.

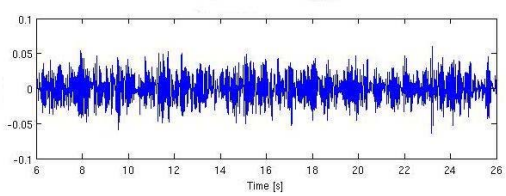

Figure 3: Raw detector noise time series

2-3. Inverse calibration

As mentioned in 2, we performed inverse calibration in FD. It essentially transforms physical strain into detector signal.

$$d_{err}(f) = R^{-1}(f)h(f)$$

So, we need inverse of transfer function $R^{-1}(f)$. According to [1], length and sensing control in S4 is modeled in the following block diagram. C, D, A are sensing function, filter, and actuation function respectively. $\gamma(t)$ is a product of optical gain $\alpha(t)$ and feedback gain $\beta(t)$ and it varies very slowly. These time-varying parameters are put into model to compensate the discrepancy due to change of optical gain and filter gain.

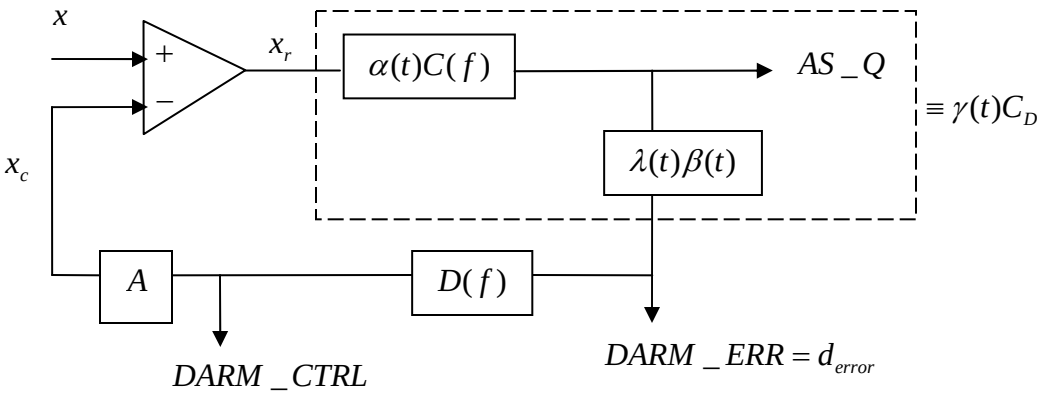

Figure 4: Block diagram of DARM model

From the above, there are some obvious relations.

$$x_r(f) = x(f) - x_c(f) \tag{11}$$

$$d_{error}(f) = \gamma(t)C_D(f)x_r(f) \tag{12}$$

$$x_c(f) = A(f)D(f)d_{error}(f) \tag{13}$$

From these relations,

$$x = \left(A(f)D(f) + \frac{1}{\gamma(t)C_D(f)} \right) d_{error} \tag{14}$$

$$\therefore R(f) = A(f)D(f) + \frac{1}{\gamma(t)C_D(f)} = \frac{1+\gamma(t)G(f)}{\gamma(t)C_D(f)} \tag{15}$$

where $G(f) = A(f)D(f)C_D(f)$, and $\gamma(t) = \alpha(t)\beta(t)$. Therefore,

$$R^{-1}(f) = \frac{\gamma(t)C_D(f)}{1+\gamma(t)G(f)} \tag{16}$$

$$d_{err}(f) = R^{-1}(f)x(f) = \frac{\gamma(t)C_D(f)}{1+\gamma(t)G(f)}x(f) \tag{17}$$

Thus, once we have $h(f)$ with arm length, artificial detector signal $d_{err}(f)$ can be created. Finally, we have the time series $d_{err}(t)$ by doing inverse Fourier transform on the frequency series.

2-4. Time-domain calibration

As mentioned in introduction, $h(t)$ is mathematically described by (2).

$$h(t) = \int_{-\infty}^{+\infty} r(t-t')d_{err}(t)dt'$$

In TD calibration we mean, $r(t)$ is not just an inverse-Fourier-transformed response function, but rather it is a digitized one using bilinear transform technique. The detail will be found in [3], so we briefly mention the technique here. As explained in previous section, response function in LIGO consists of sensing function, filter, and actuation function. And, each of them can be expressed by ratio of polynomials of s, or 'zeros and poles' in Laplace domain. Let's call a transfer function in Laplace domain, $H(s)$.

$$H(s) = \frac{b(N)s^N + b(N-1)s^{N-1} + \cdots + b(1)s + b(0)}{a(M)s^M + a(M-1)s^{M-1} + \cdots a(1)s + a(0)} = \frac{\sum_{k=0}^{N} b(k)s^k}{\sum_{l=0}^{M} a(k)s^l} \tag{18}$$

By doing bilinear transform,

$$s = \frac{2}{t_s}\left(\frac{1-z^{-1}}{1+z^{-1}}\right) \tag{19}$$

we get transfer function in 'z-domain'.

$$H(z) = \frac{Y(z)}{X(z)} = \frac{\sum_{k=0}^{P} c(k)z^{-k}}{1-\sum_{l=1}^{Q} d(l)z^{-l}} \tag{20}$$

t_s is sample period. Then, we get time-domain expression,

$$\begin{aligned} &y(n) = c(0)x(n) + c(1)x(n-1) + \cdots + c(P)x(n-P) \\ &+ d(1)y(n-1) + d(2)y(n-2) + \cdots + d(Q)y(n-Q) \end{aligned} \tag{21}$$

From (5), assuming we have digital-filtered expression of inverse sensing function, filter, and actuation function, $H_{C^{-1}}$, H_D, and H_A respectively,

$$x(t_n) = H_A\{H_D[d_{err}(t_n)]\} + \frac{1}{\gamma(t)}H_{C^{-1}}[d_{err}(t_n)] \tag{22}$$

Therefore,

$$r(t) = H_A H_D + \frac{1}{\gamma(t)} H_{C^{-1}} \qquad (23)$$

We compare $r(t)$ with original response function in frequency domain. Plotted in figure 5 and figure 6 are the response function and the relative difference. Their difference is less than a few percent in entire frequency region.

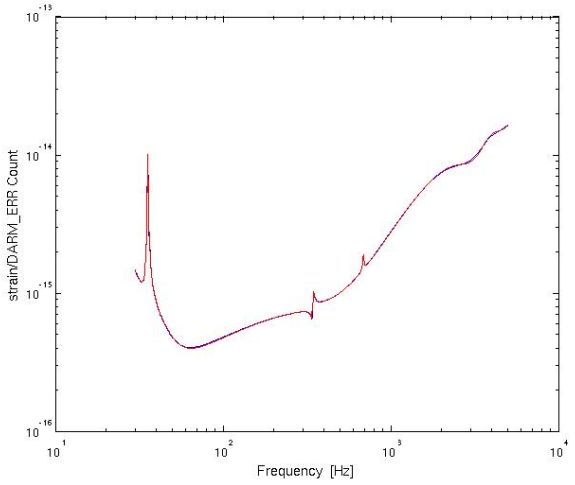

Figure 5: Response function (Red – official, Blue – digitized)

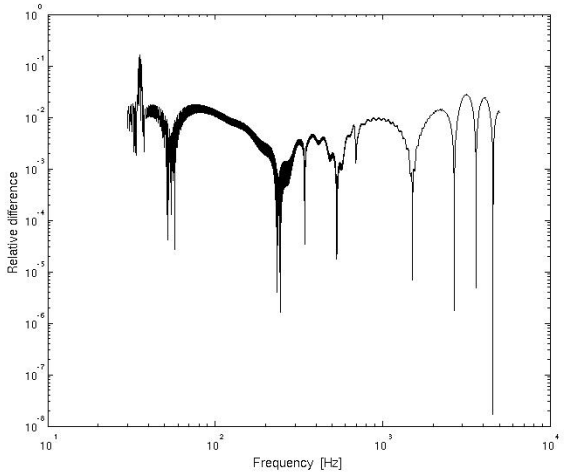

Figure 6: Relative difference of the two response functions

2-5. Reconstruction of injected signal

Applying TD code to both raw error signal $d_{err}(t)$ and fake gravitational wave signal '$d_{err}(t) + d_{err}(t)_{SG}$', we get two physical strain signals as shown below.

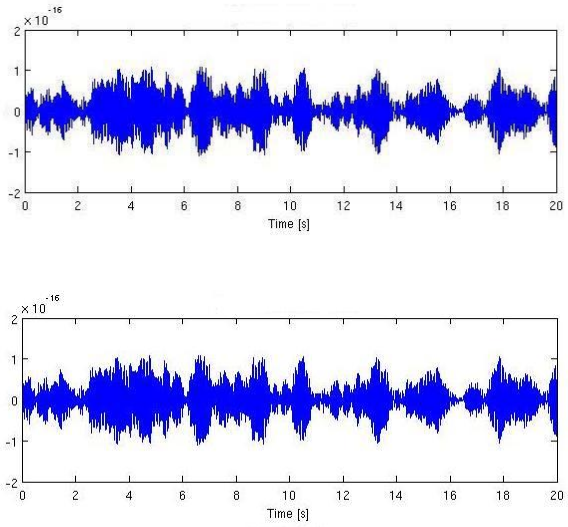

Figure 7: TD calibrated signals

Figure 7 shows error strain signal $h(t)_{err}$ (top) and the combined strain $h(t)_{err+SG}$ (bottom). They look identical in this scale since amplitude of the added sine-Gaussian is small compared to the noise. Subtracting $h(t)_{error}$ from $h(t)_{error+SG}$, we reconstruct injected signal $h(t)_{rec}$.

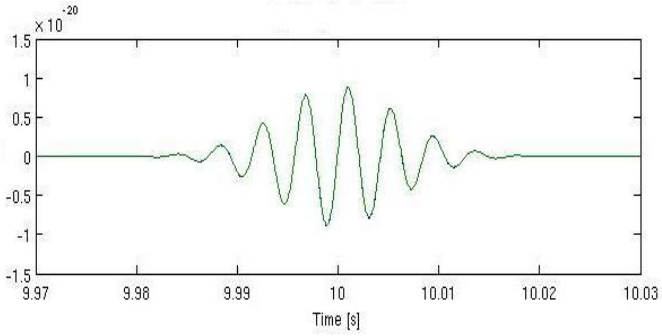

Figure 8: Reconstructed signal

Figure 8 shows reconstructed signal. Looking at the profile, it looks like sine-Gaussian. We discuss how close the signal is to the original sine-Gaussian in the next chapter.

3. Results

Figure 9 shows both the original SG curve (red) and reconstructed one (blue) in frequency domain, whose center frequency and the strength are $f_0 = 235Hz, h_0 = 0.9\times10^{-20}$ respectively. We see good agreement around the center frequency and poor agreement outside the region. Before addressing in detail, let's take a look at the case when we have much weaker SG signal, whose amplitude is $h_0 = 5.0\times10^{-30}$ (figure 10). As seen clearly, original curve looks as if it shifted downwardly while reconstructed curve looks remaining still. In other words, blue curve cannot follow the shift of the original curve. So, we can think of level of this 'static' blue curve as numerical noise coming from the procedure discussed in chapter 2. From this behavior, one can easily imagine that no overlap will occur if we lower amplitude more. The error never comes from detector noise since we subtract noise component of DARM_ERR in reconstruction process. Given this knowledge, we roughly define 'signal region' where amplitude is large enough so that we can compare the two curves. From figure 10, we can roughly define 'above $10^{-27}[s]$' as our signal region. What we want to see in this study is accuracy of TD calibration method in the signal region. As we go outside the region in either side, the discrepancy between the two curve increases rapidly, but we do not care about it. Using several different center frequency-SGs, we will be able to have signal region in entire frequency region. As we will see later, as long as relative difference of different curves overlaps, we have freedom to choose on amplitude and strength of sine-Gaussians.

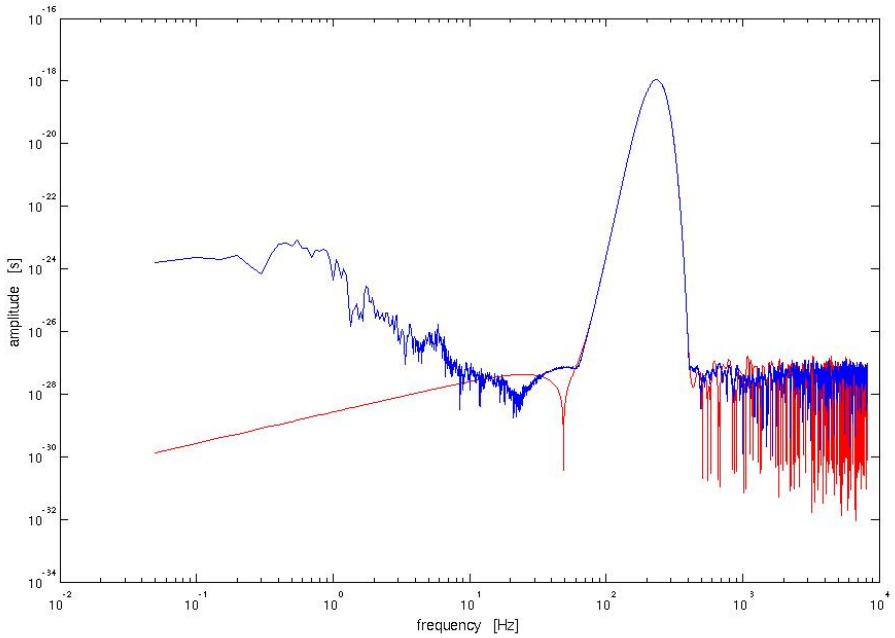

Figure 9: SG curves in frequency domain (Red-original, Blue- reconstructed)

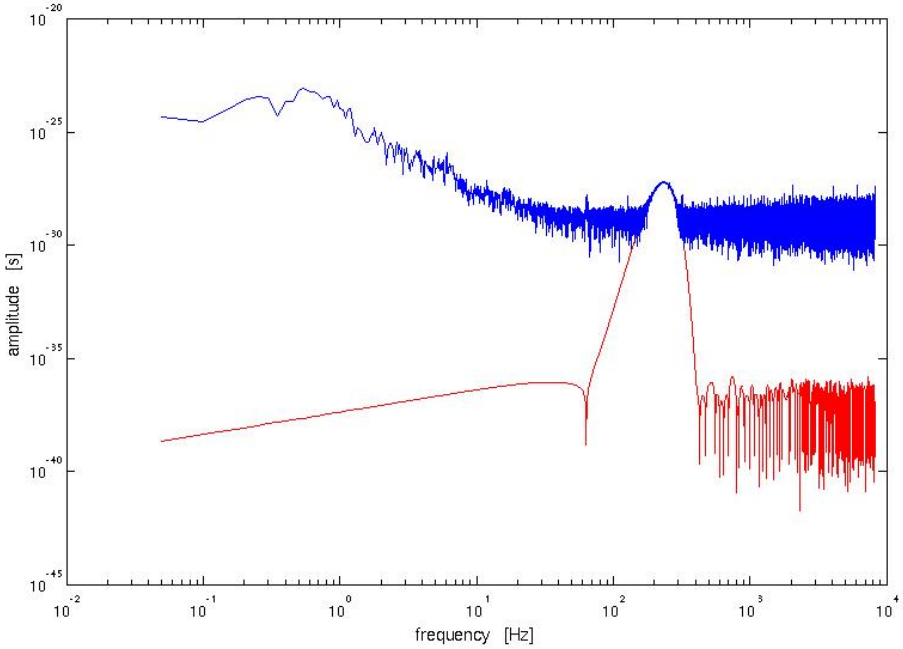

Figure 10: SG curves in frequency domain (weak amplitude)

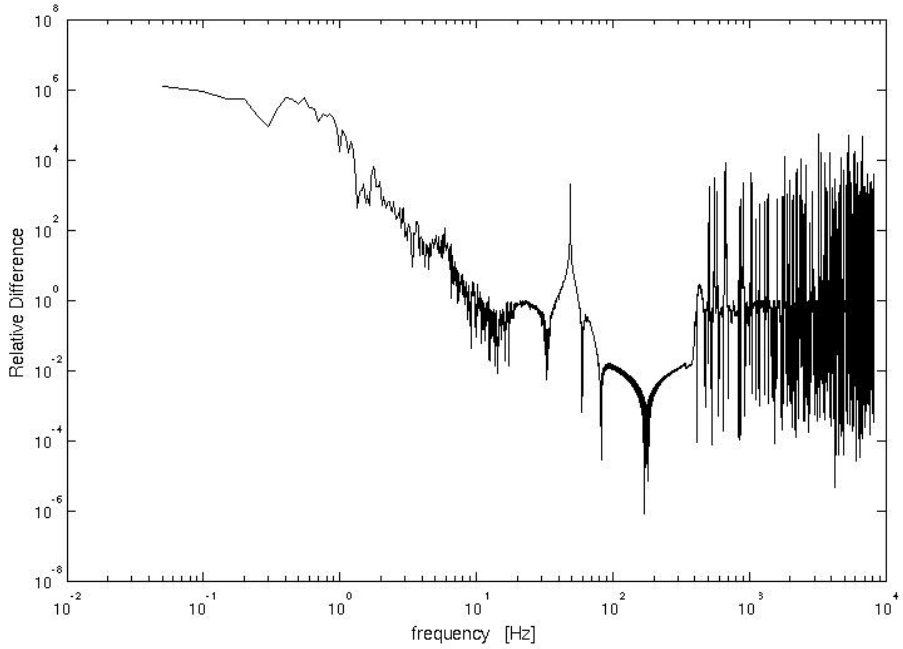

Figure 11: Relative difference (235Hz)

Shown is relative amplitude difference in log-log scale defined by $\log\left|\left(\left|h_{ORG}\right|-\left|h_{REC}\right|\right)/\left|h_{ORG}\right|\right|$.
From this graph, we define the signal region from 80 Hz to 360 Hz. Next graph (figure 12) is zoomed one in linear scale. Agreement of the two method is within 1.5% here.

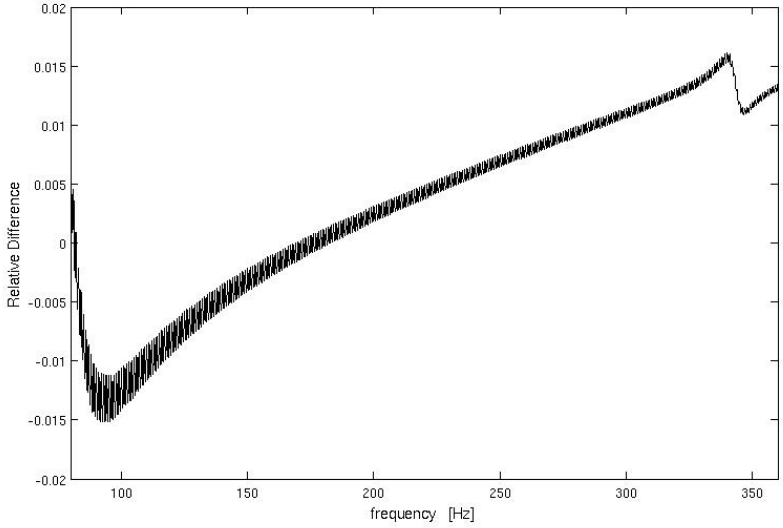

Figure 12: Zoomed relative difference (235Hz)

Phase curve, phase difference, and the zoomed phase difference are plotted in figure 13, 14, and 15 respectively.

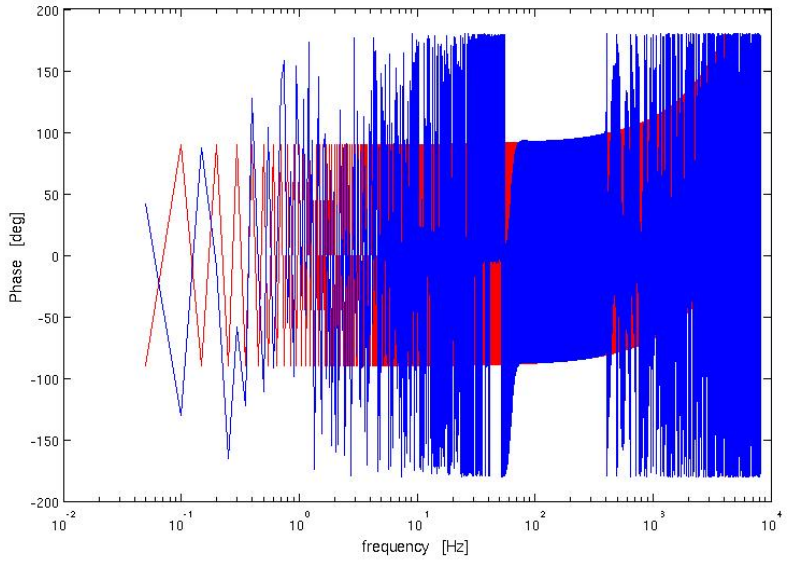

Figure 13: Phase (Red-original, Blue-reconstructed)

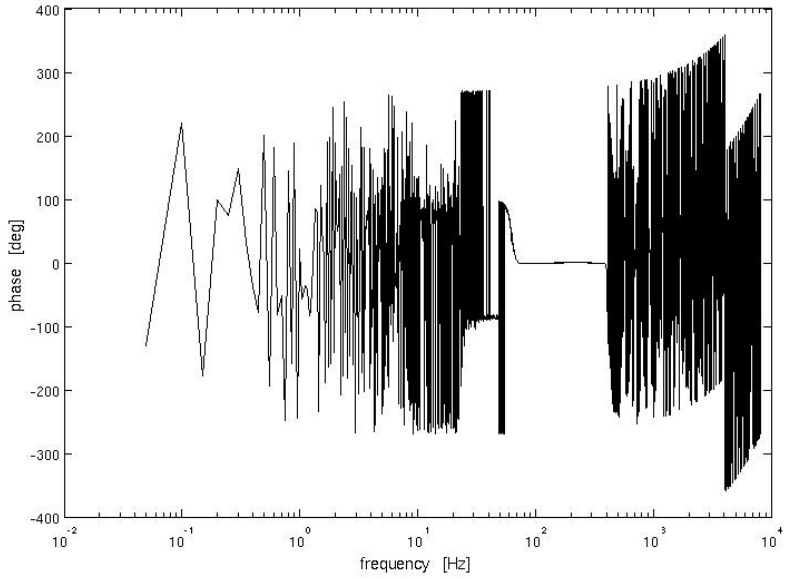

Figure 14: Phase difference

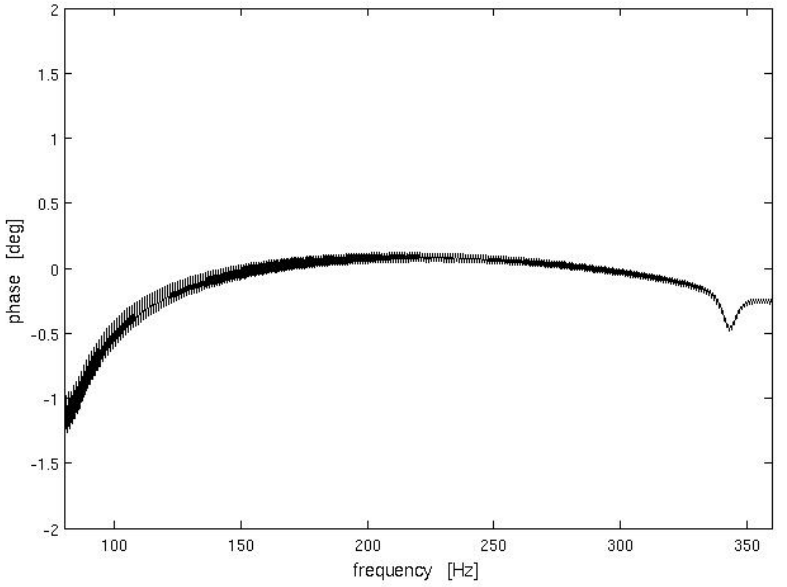

Figure 15: Zoomed phase difference

Phase difference in the signal region is from -1.2 deg to 0.1 deg, which is reasonably good.

We checked the same test for six different SG curves listed in table 1. Then, we plotted those things together in figure 16. As we can see in the plot, each curve of different SG curves is connected smoothly in both amplitude and phase. Since the six curves have all different center frequency and some of them even have different amplitude (strength), the smoothness supports the idea that we have freedom to define 'signal region'. Also, the smoothness is telling us that this result does not depend on the choice of injected signals. Namely, we could get the same result by using infinite number of sine curves, for example. In this sense, our choice of SG curve was analog of using 'swept-sine' curve in taking frequency response in some experiment. From the plot, we conclude accuracy of TD calibration is within 3.2% in amplitude and 3 deg in phase through entire frequency range (40 Hz – 6000 Hz).

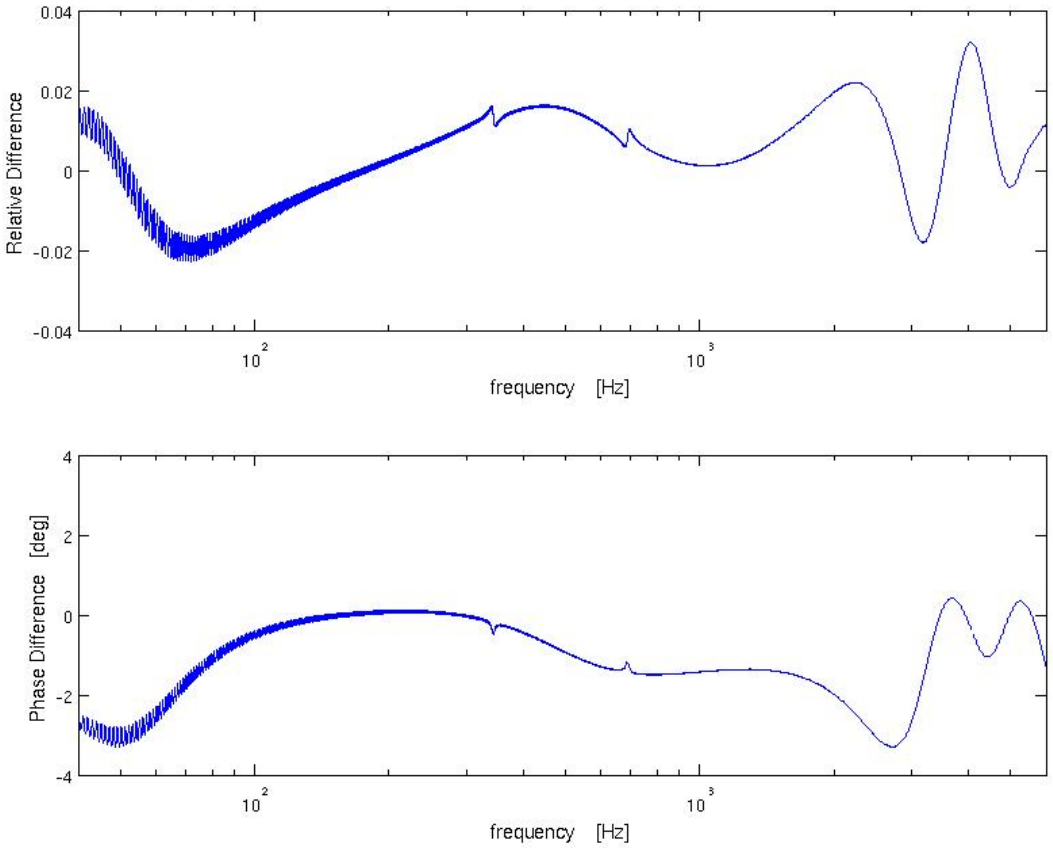

Figure 16: Difference between the two methods

Finally, we compare this result with pure response-function-difference between two methods. Namely, we plot figure 16 (red) and figure 6 (blue) together in figure 17. When we do this, absolute value taken in figure 6 is given up. The difference is at most about 1% and the trend is

almost identical. But, essentially these curves should be identical judging from equation (1) and (2). Main cause of this discrepancy must be error in inverse calibration procedure.
Profile of figure 16 and figure 17 depend on how we digitize transfer function, of course. And, this study tells us that we need to watch just difference between digitized response function and official response function in order to argue difference between TD and FD method.

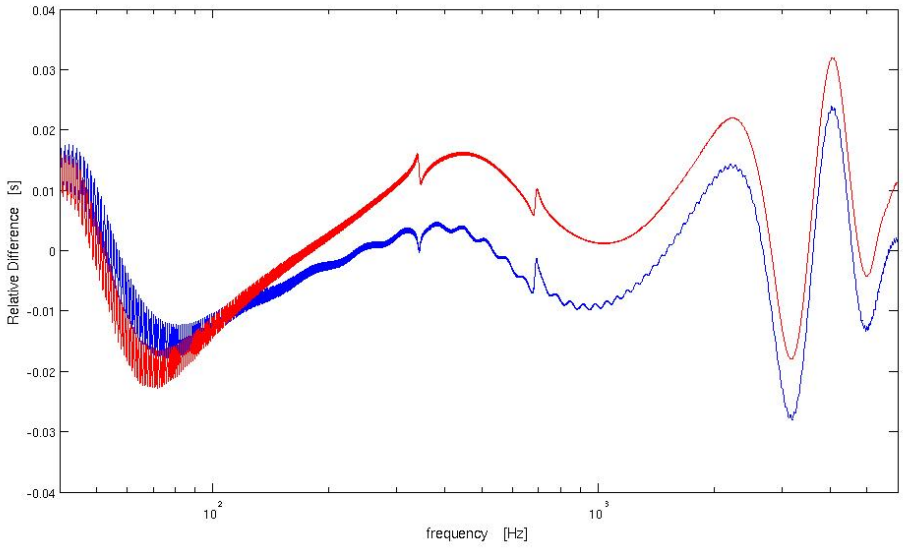

Figure 17: Comparison of two curves
(Red – same as figure 16, Blue – difference between R(f) and Fourier transformed R(t)

4. Conclusion

We showed a method of TD validation using six different sine-Gaussian curves. TD calibration agrees to FD calibration within 3.2% in amplitude and 3deg in phase in very broad frequency range (from 40Hz to 6000Hz). We also showed it should be enough to compare digitized response function with the official response function in order to see the difference in two calibration methods.

5. Acknowledgement

EH thanks Peter R. Saulson for initiating this project and his support on various aspects. EH also thanks Keith Thorne for providing his useful codes and people in calibration team for their support. Especially, Mike Landry gave EH a lot of lectures with patience. We both also thank Sergey Klimenko for introducing his idea on this TD validation method. Without their help, this project would not have been done.

6. Reference

[1] A. Dietz, J. Garofoli, G. Gonzalez, M. Landry, B. O'Reilly, M. Sung, Calibration of the LIGO detectors for S4, LIGO-T00262-00-D

[2] X. Siemens, B. Allen, J. Creighton, M. Hewitson, M. Landry, Making $h(t)$ for LIGO, gr-qc/0405070

[3] Richard G. Lyons, Understanding Digital Signal Processing, Prentice Hall

[4] Communication via emails with Sergei Klimenko